Single Shot Multi-Dimensional Imaging using Magnetic Field Monitoring and including Maxwell Terms

Frederik Testud[1], Daniel Gallichan[2], Kelvin J. Layton[3], Anna M. Welz[1], Christoph Barmet[4], Chris A. Cocosco[1], Jürgen Hennig[1], Klaas P. Pruessmann[4], and Maxim Zaitsev[1]

[1]Medical Physics, University Medical Center Freiburg, Freiburg, Germany, [2]Centre d'Imagerie BioMédicale, Ecole Polytéchnique Fédérale de Lausanne, Lausanne, Switzerland, [3]Electrical & Electronic Engineering, University of Melbourne, Parkville, Victoria, Australia, [4]Institute for Biomedical Engineering, University and ETH Zürich, Zürich, Switzerland

Introduction: Non-linear non-bijective PatLoc (parallel acquisition technique using localized gradients) encoding has been proposed [1] to potentially minimize peripheral nerve stimulations by using e.g. two hyperbolic or one elliptic paraboloid field. Single shot multi-dimensional imaging as 4-Dimensional Radial In/Out (4D-RIO) [2] or North West Echo Planar Imaging (NW-EPI) [3] combine linear and PatLoc gradient fields to exploit the variability of spatial resolution and avoids the total resolution loss in the centre of the field of view (FOV). The image reconstruction is sensitive to field drifts, eddy currents, hardware delays and concomitant fields leading to blurring, geometric distortions and ghosting. Magnetic Field Monitoring (MFM) [4,5] addresses these issues by estimating the trajectory from field probes' signal phase. In this work, the analytical form of Maxwell terms for three linear (XG_x, YG_y, ZG_z), two hyperbolic (XYG_a and $(X^2\text{-}Y^2)G_b$) and one elliptic (Z^2G_c) paraboloid magnetic fields is presented with G_x,…, G_c their respective amplitudes. Their spatial dependencies are used to build a different set of basis functions (θ_1) from the real spherical harmonics (θ_0). A field camera is used for trajectory calibration. Phantom and in-vivo NW-EPI and 4D-RIO measurements were performed and reconstructed with the nominal and measured trajectories using the basis θ_0 and θ_1.

$$\vec{k}(t) = (\mathbf{P}^T\mathbf{P})^{-1}\mathbf{P}^T[\vec{\phi}(t) - \vec{\omega}_{\text{ref}}t - \vec{\phi}_0] \qquad \text{(Eq. 1)}$$

$$B_c = \left\|\vec{B}(\vec{r})\right\| - B_z \qquad \text{(Eq. 2)}$$

$$\begin{aligned} B_c = \frac{1}{2B_0} \big[& \big(\big(4\alpha^2G_c^2 - 8G_c^2\alpha - 8\alpha G_cG_a + 8G_cG_a + \\ & +4G_b^2 + 4G_c^2 + 4G_a^2\big)\, y^2 + \\ & + \left(-4\alpha G_cG_x + 4G_yG_b + 4G_xG_a\right) x + \\ & + \left(4G_xG_b - 8G_cG_bx - 4G_cG_y - 4G_yG_a + 4G_c\alpha G_y\right) y + \\ & + \left(4G_a^2 + 4\alpha^2G_c^2 + 4G_b^2 - 8\alpha G_cG_a\right) x^2 + G_y^2 + G_x^2\big)\, z^2 + \\ & + \big(\big(4\alpha^2G_zG_c - 8G_zG_c\alpha + 4G_zG_c + 4G_zG_a - \\ & +4G_z\alpha G_a + 4gG_b\big)\, y^2 + \\ & + \left(2G_yg - 2Gz\alpha G_x\right) x + \left(4\alpha^2G_zG_c + 4gG_b - 4G_z\alpha G_a\right) x^2 + \\ & + \left(\left(-4G_zGb - 4gG_c\right) x - 2G_zG_y + 2gG_x + 2G_zG_y\alpha\right) y\big)\, z + \\ & + \left(Gz^2 - 2z^2\alpha + G_z^2\alpha^2 + g^2\right) y^2 - \\ & 2xgyG_z + \left(G_z^2\alpha^2 + g^2\right) x^2\big] \end{aligned} \qquad \text{(Eq. 3)}$$

basis θ_0	basis θ_1
1	1
X	X
Y	Y
Z	Z
XY	XY
ZY	ZY
$3Z^2\text{-}(X^2+Y^2+Z^2)$	X^2+Y^2
XZ	$Z(X^2\text{-}Y^2)$
$X^2\text{-}Y^2$	$X^2\text{-}Y^2$
$Y(3X\text{-}Y^3)$	ZX^2
XYZ	XYZ
$Y(5Z^2\text{-}(X^2+Y^2+Z^2))$	Y^2Z^2
$Z(5Z^2\text{-}3(X^2+Y^2+Z^2))$	X^2Z^2
$X(5Z^2\text{-}(X^2+Y^2+Z^2))$	ZY^2
$X(X^2\text{-}3Y^2)$	Z^2X

Tab. 1: Basis functions used for trajectory estimation.

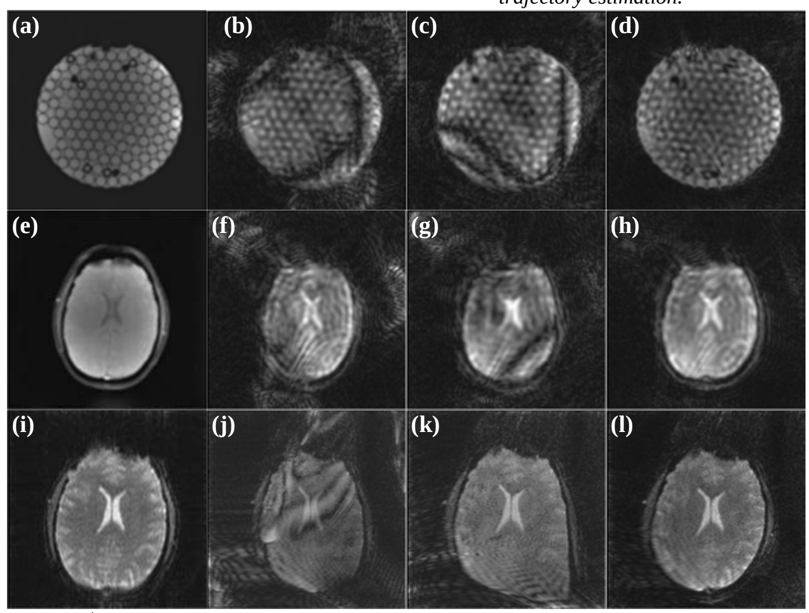

Fig. 1: 1st column shows reference images using linear gradients. (a) and (e) are gradient echo images from the acquired field maps and (i) is an echo planar image from the same slice. 2nd, 3rd and 4th column are reconstructed images using the nominal trajectory, using basis θ_0 (spherical harmonics) and θ_1 (including Maxwell terms), respectively. 1st and 2nd line shows 4D-RIO phantom and in-vivo images, the 3rd line NW echo planar images.

Theory: The measured field probes' phases $\vec{\phi}(t)$ (Eq. 1) reflect the magnetic field evolution at their positions (x, y, z) with respect to the applied linear gradients. The initial value of the phases $\vec{\phi}_0$ and the linear drift $\vec{\omega}_{\text{ref}}(t)$ has to be subtracted. The trajectory $\vec{k}(t)$ is estimated from the unwrapped phases in the least square sense according to the basis functions (Tab. 1) set in the probing matrix **P** using the field probes' position. The Maxwell terms of the hyperbolic paraboloid fields are estimated as in [7] for three linear, two paraboloid and one elliptic gradient (Eq. 2-3). g and α are constants obtained in the derivation of B_c. The spatial dependencies of B_c (Eq. 3) are used to build the basis θ_0 (Tab. 1).

Methods: Measurements were performed on a 3T Tim TRIO MR scanner (Siemens Healthcare, Erlangen, Germany). The PatLoc fields are produced by a head gradient coil insert [6] producing two parabolic hyperboloids magnetic fields of the type XY and $X^2\text{-}Y^2$ rotated around the z-axis by $\pi/8$. The corresponding concomitant field is obtained by setting G_c=0 and take the above rotation into account (Eq. 3). The field camera consists of 16 unshielded H^1 field probes [5] approximately distributed on a spheroids' surface ($\varnothing x \approx \varnothing y \approx 18$cm and $\varnothing z \approx 14$cm) placed inside the head coil and connected to the spectrometer of the scanner. The separate transmit chain [3] is controlled via trigger signals from the scanner. NW-EPI (FOV: 220×220×3 mm^3, 128×128 px^2) and 4D-RIO (FOV: 256×256×3 mm^3, 128×128 px^2) images were acquired. Image reconstruction using conjugate gradient with the full encoding matrix computed on demand on Graphics processor units [8] and data analysis are performed offline in MATLAB (The Mathworks, Natick, AM, USA).

Results & Discussion: Reconstructed phantom and in-vivo images using the nominal trajectory, the measured trajectory fitted to basis θ_0 and θ_1 are shown in Fig. 1. Last column in Fig. 1 depicts fewer artefacts and signal voids as in the images reconstructed using the nominal or estimated trajectory from basis θ_0 (Tab. 1), which do not take Maxwell terms' spatial dependencies (Eq. 3) into account. However, small artefacts such as ringing and geometric distortions are still present in Fig. 1 (d), (h) and (l), possibly due to the assumption of perfectly quadratic source fields A and B for the derivation of the Maxwell terms.

Conclusion: Successful single shot multidimensional imaging with 4D-RIO or NW-EPI is possible with trajectory calibration using MFM. Image quality improvements are obtained when taken the Maxwell terms' spatial dependencies into account.

References: [1] J. Hennig et al. 2008 MAGMA 21; [2] D. Gallichan et al. 2012 Proc. ISMRM 292; [3] K. Layton et al. 2012 MRM early view; [4] C Barmet et al. MRM 2008 60; [5] B. Wilm et al. 2011 MRM 65; [6] A. Welz et al. 2009 Proc. ISMRM 3073; [7] M. Bernstein et al. 1998 MRM 39; [8] C. Cocosco et al., GTC 2012, S#0348;

Acknowledgments: This work has been supported by the INUMAC project supported by the German Federal Ministry of Education and Research, grants #01EQ0605 & #13N9208.